

# Influence of strain rate on deformation and failure behavior of sheet metals under shear loading

S. Klitschke, A. Trondl, F. Huberth

Fraunhofer Institute for Mechanics of Materials IWM, Freiburg, Germany

## 1 Abstract

In order to improve the reliability of deformation and failure prediction of automotive lightweight constructions in real crash situations, appropriate input data for crash simulations are necessary which represent the material behavior under high strain rates and complex multiaxial loading situations. Especially under shear dominated loading failure is difficult to reach and there is still a lack of information concerning the strain rate dependency under these loading conditions. Therefore an experimental procedure for strain rate dependent shear tension tests on sheet metals was developed which bases on asymmetrical notched shear tensile specimen geometries without surface processing. The specimen design of the shear zone was optimized by varying the shear length dependent on the sheet thickness and the notch position dependent on material data of uniaxial tension tests. For different advanced high strength steels (AHSS) numerical and experimental investigations were performed regarding the evolution of load paths in the shear zone and near the notch region as well as the failure location. Based on these experimental results and related numerical simulations recommendations are derived for an optimized design of asymmetrical notched shear tensile specimens. These recommendations are dependent on the sheet thickness and on material properties. The experiments should be carried out comparable to strain rate dependent flat tension tests with an appropriate mounting. The suggested specimen design procedure is validated by experiments on steels in a wide range of strength as well as on exemplary batches of aluminum and copper. The shear characterization for AHSS results in large strain values in the shear zone up to failure under quasi-static loading with a significant negative strain rate effect. These experimental results of improved strain rate dependent shear characterization can be used for enhanced failure prediction in the future.

KEYWORDS: shear characterization, strain rate, notched shear tensile specimen, shear failure strain

## 2 Introduction

Shear failure is a very critical loading state in terms of crash worthiness because failure occurs suddenly without previous necking or observable instability. Several investigations in the past have shown, that for different metallic materials shear failure strains are significantly lower under crash loading than under quasi-static loading based on a gauge length scale of about 100  $\mu\text{m}$  and larger [1,2,3,4]. This effect has a significant impact on the strain rate dependency of the failure prediction in the shear region and should be considered in crash simulations. For a reliable detection of strain rate effects under shear loading a systematic experimental procedure with suitable shear specimens is essential and should work for quasi-static tests as well as for dynamic loading velocities. For sheet metals under quasi-static loading the realization of shear failure is difficult to reach, because of superimposed tension loading in some parts of the specimen like in notch regions. Therefore many investigations concentrate on the optimization of several shear specimen geometries with different advantages and disadvantages, for example butterfly specimens, round torsion specimens, sheet torsion specimens, notched shear tensile specimens, miyauchi specimens and others [2,5,6,7,8,9,10,11]. In this paper investigations for an optimized strain rate dependent shear characterization are presented with focus on sheet metals of advanced high strength steels (AHSS). The design of the optimized shear specimen is material dependent and based on technical values from uniaxial tension tests. The following criteria are defined as important:

1. The main (initial) rupture should occur in the shear zone under shear dominated loading states instead of regions under tensile dominated loading conditions
2. Triaxiality  $\eta \sim 0$  in the shear zone
3. Proportional strain paths in the shear zone
4. Characterization procedure suitable for quasi-static and dynamic loading

5. No surface processing of the specimen (e.g. thinning)
6. Shear zone visible for video recording and DIC evaluation
7. Simple and cost efficient specimen extraction

Concerning those criteria the asymmetric notched shear tensile specimen was chosen as a suitable geometry with optimization potential by varying geometry parameters in the shear zone. This geometry can be tested quasi-statically and dynamically with the same test set up as it is used for flat tension tests. Additionally there already exist experiences in strain rate dependent characterization with this kind of specimen geometry [4,8]. A disadvantage of the notched shear tensile specimen is the tendency to failure initiation in the notch region under tension dominated loading states. The probability of notch failure can be reduced by varying the design of the shear zone dependent on the material behavior. As a basic geometry for the optimization procedure the asymmetric notched shear tensile specimen shown in Figure 1 left [4] was chosen. The modifiable parameters are the notch radius  $R$ , the shear length  $L$  and the notch angle  $\xi$  (notch overlap), see Figure 1 right. A negative notch overlap angle is proposed in [12] and reduces the triaxiality in the shear zone. A goal is to establish a simple shear characterization procedure for different steel sheet materials under the constraint to use less number of parameters as possible to induce shear dominated deformations and failure.

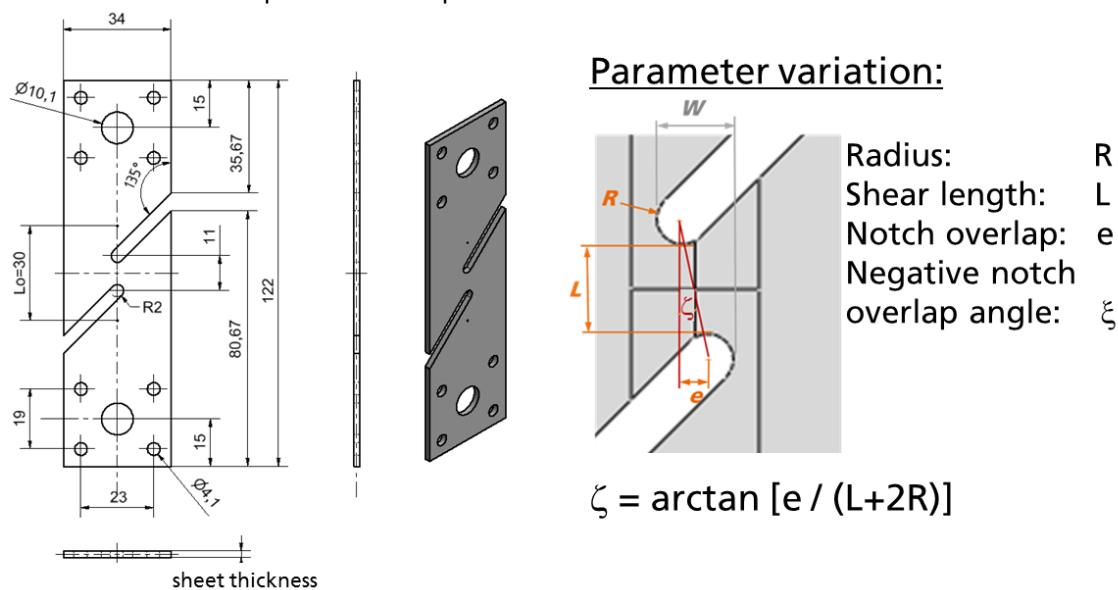


Fig.1: Basic geometry for notched shear tensile specimen (left) and variation of shear zone parameters (right).

The investigations in this work were performed on dualphase steels, complexphase steels and one microalloyed steel with sheet thicknesses  $t$  between 1 mm and 2 mm, documented with the technical values perpendicular to the rolling direction in Table 1.

Material	sheet thickness $t$ [mm]	$R_{p0.2}$ [MPa]	$R_m$ [MPa]	$A_g$ [%]	$A_{20mm}$ [%]	$n_{2-Ag}$	Z [%]
HX340LAD	1.5	390	461	17.4	35.6	0.149	62.5
HCT980X+Z110MB	1.5	683	1007	10.3	18.5	0.132	35.1
HCT980XG	1.4	759	1049	7.1	13.4	0.081	33.5
HCT780C	1.0	746	946	7.2	12.7	0.087	48.2
HCT780C	1.5	689	878	8.4	17.4	0.094	50.5
HCT980C	1.0	941	1039	4.6	10.8	0.045	45.4
HCT980C	1.5	890	1003	5.1	13.7	0.057	53.9
HCT980C	2.0	923	1009	4.6	15.7	0.047	58.7

Table 1: Investigated materials with technical values (perpendicular to rolling direction).

The deformation and failure behavior under uniaxial tension is investigated with quasi-static tests on smooth tensile specimens with a parallel length of  $L_c = 25$  mm proposed in [13] as a suitable geometry for a wide range of test speeds (Figure 2 left). The obtained stress-strain curves for the investigated materials are shown in Figure 2 right).

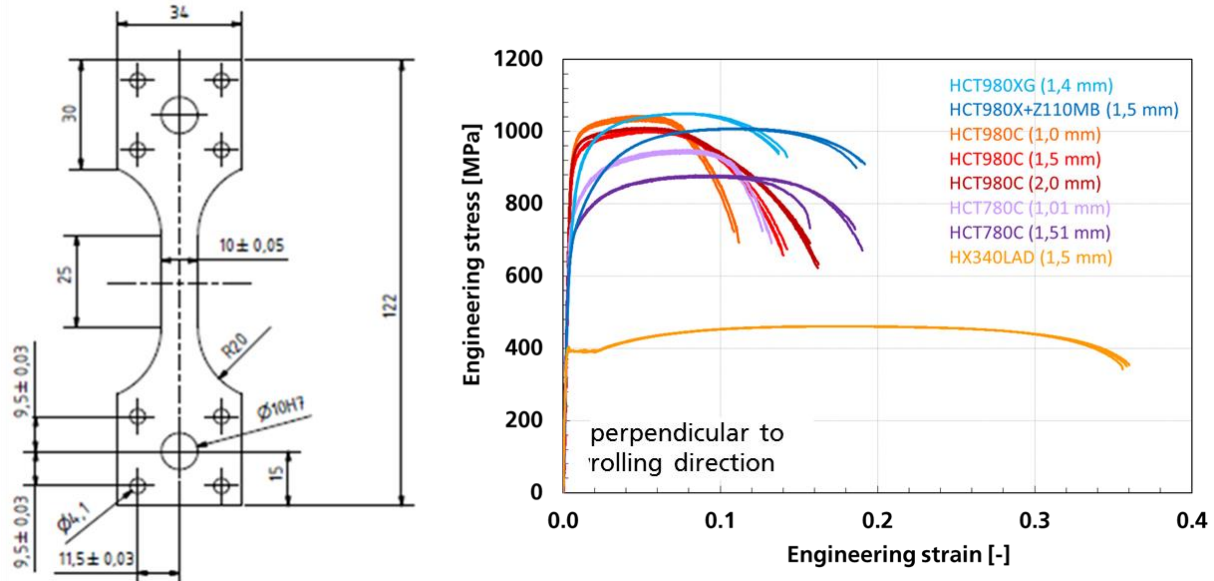


Fig.2: Specimen geometry for uniaxial tension tests (left) and Engineering stress strain curves for the investigated materials perpendicular to the rolling direction (right).

### 3 Numerical investigations

The shear parameter optimization was performed with LS-Dyna 10.0.0 [14] with fully integrated solid elements (elf2) with an element size of 0.1 mm in the shear zone and 10 elements over the sheet thickness. The material plasticity was described by Mat\_024 [14]. The flow curves were determined by extrapolating the experimental true stress strain curves of the quasi-static flat tension tests and optimized by reverse engineering. The calculations for the shear parameter optimization were carried out under quasi-static loading conditions with the specimen geometry shown in Figure 1 left by varying the shear parameters  $R$ ,  $L$  and  $\xi$ . For an assessment of the specimen geometry concerning the suitability for shear characterization the following two criteria are identified as relevant:

1. The ratio between strains in the shear zone and strains in the notch region should be as large as possible to avoid failure initiation in the notch region. For the major part of the deformation process the strains in the shear region should be larger than those in the notch region.
2. The variations of the load path in the shear zone should be less as possible and the triaxiality should be close to zero.

A numerical preliminary study has shown that  $R = 1$  mm leads to significant lower strains in the notch region compared to the initial notch Radius of  $R = 2$  mm. To reduce the number of parameters, the following simulations were performed with  $R = 1$  mm. In the succeeding procedure the influence of  $L$  and  $\xi$  on the strains and load paths in the shear zone were analyzed with regard to the above mentioned two criteria. In Figure 3 the analyzed elements on the surface of the specimen are shown exemplarily. In the shear zone an element in the center of the localization zone is chosen. In the notch region two elements are analyzed. One element in the notch root, where the triaxiality changes very sharply from shear loading to multiaxial tension loading, and one element in the center of the notch, where strain localization under tension loading occurs. For those chosen elements the strain and triaxiality evolution was analyzed for the whole deformation process up to a strain level in the shear zone of about 1.5.

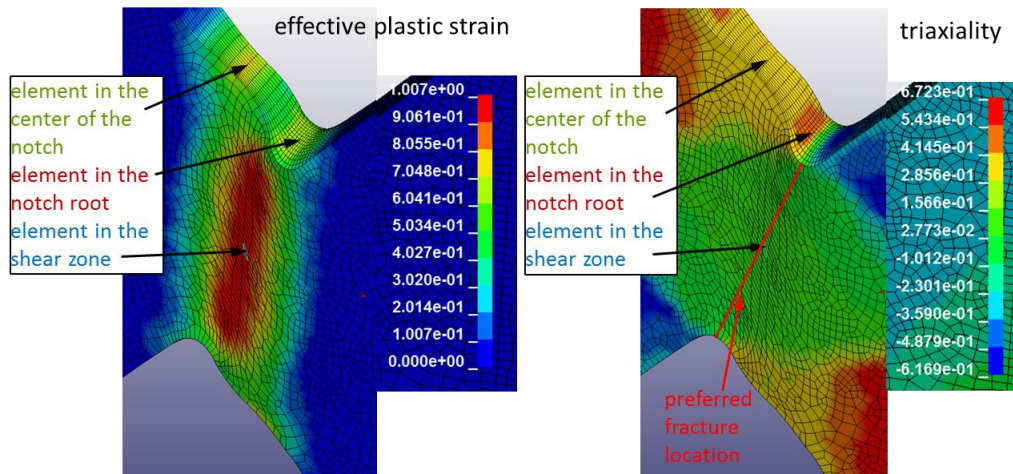


Fig.3: Effective plastic strain (left) and triaxiality (right) on the surface of the shear zone with analyzed elements (HCT980XG,  $R = 1\text{ mm}$ ,  $L = 4\text{ mm}$ ,  $\xi = -10^\circ$ )

The influence of  $\xi$  on the effective plastic strain evolution is demonstrated in Figure 4 for HCT980XG and a shear length of  $L = 4\text{ mm}$ . The specimen without notch overlap ( $\xi = 0^\circ$ ) shows significant larger strains in the notch root compared to the specimen with a negative notch overlap of  $\xi = -10^\circ$ . The impact of  $\xi$  on the load path is shown in Figure 5 for an element in the shear zone far away from the specimen surface. With increasing negative notch overlap the load path is shifted to lower triaxialities.

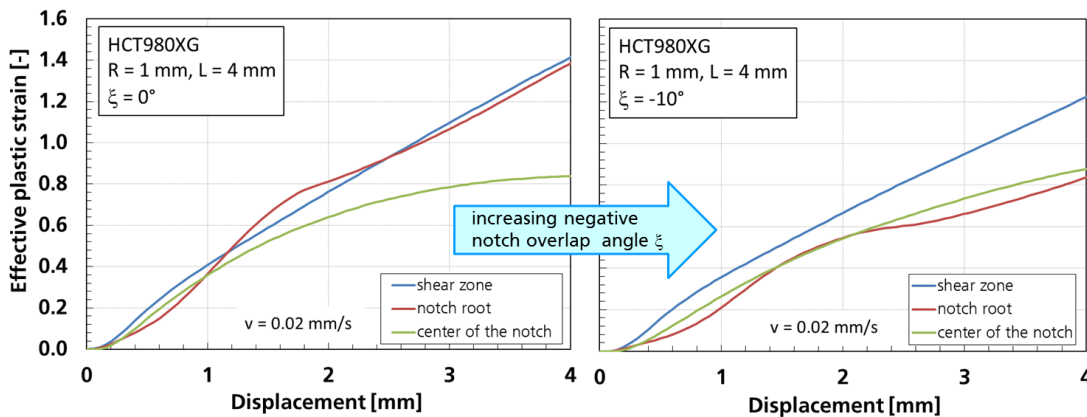


Fig.4: Evolution of effective plastic strain in the shear and notch region for HCT980XG,  $L = 4\text{ mm}$ ,  $R = 1\text{ mm}$ ,  $\xi = 0^\circ$  (left) and  $\xi = -10^\circ$  (right)

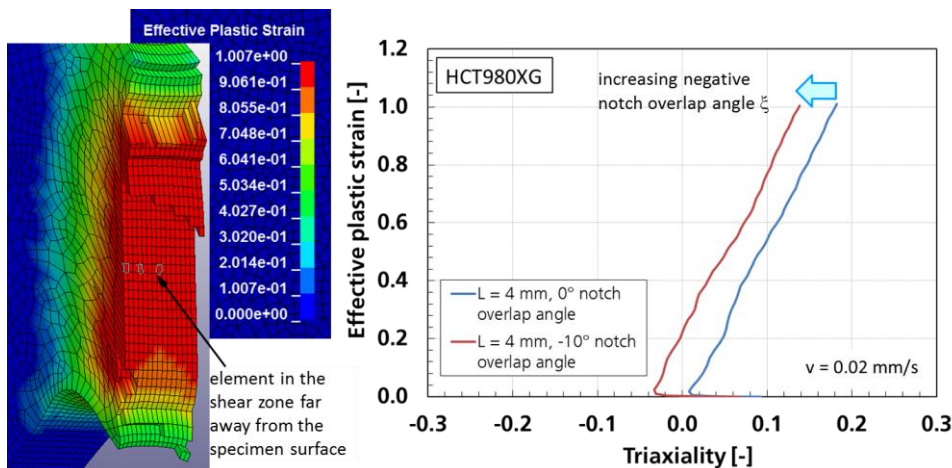


Fig.5: Effective plastic strain over the specimen thickness (left) and influence of negative notch overlap angle  $\xi$  on the load path in the shear region (right), HCT980XG,  $L = 4\text{ mm}$ ,  $R = 1\text{ mm}$

The influence of the shear length  $L$  on the effective plastic strain evolution and on the load path is demonstrated in Figure 6 exemplarily for HCT980C with a sheet thickness of  $t = 1$  mm and with  $\xi = -10^\circ$ . A reduction of the shear length leads to a decrease of strain in the notch root and to larger triaxialities in the shear zone.

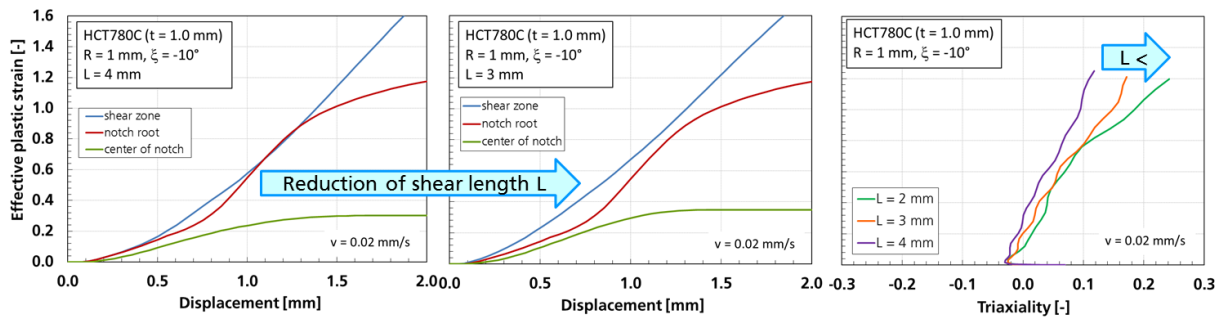


Fig.6: Evolution of effective plastic strain in the shear and notch region (left:  $L = 4$  mm, middle:  $L = 3$  mm) and load path for three shear lengths (right), HCT780C,  $t = 1$  mm,  $R = 1$  mm,  $\xi = -10^\circ$

For a sheet thickness  $t$  of 1.5 mm and 1.4 mm the geometry with  $R = 1$  mm,  $L = 4$  mm and  $\xi = -10^\circ$  showed the best results for HCT980C, HCT780C and HCT980XG. To investigate the influence of  $t$  on the optimized shear zone parameters additional calculations were performed for HCT980C with  $t = 1.0$  mm,  $t = 1.5$  mm and  $t = 2.0$  mm with this appropriate geometry and therefore with different normalized shear length related to the sheet thickness ( $L/t$ ). Results of these simulations are shown in Figure 7. With increasing sheet thickness and decreasing  $L/t$  the strains in the notch root decrease compared to the strains in the shear zone and the triaxiality simultaneously tends to larger values in the shear zone. Therefore thin sheets of steel require a smaller shear length than thicker ones.

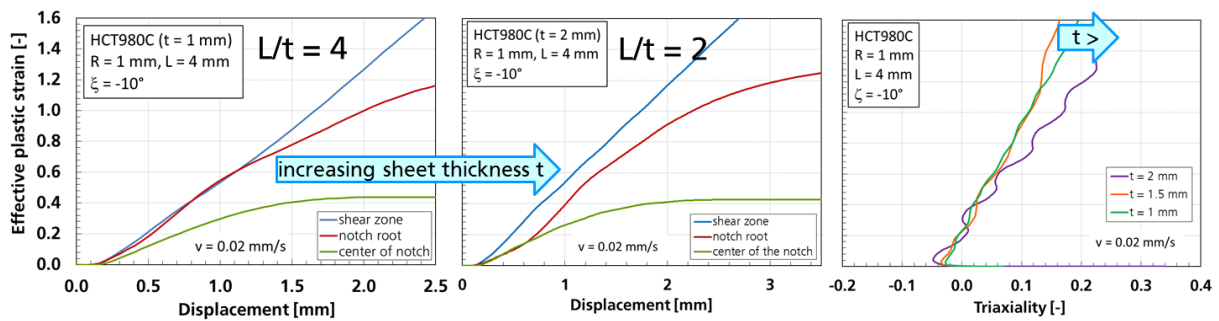


Fig.7: Evolution of effective plastic strain in the shear and notch region (left and middle) and load path (right) for different sheet thicknesses, HCT980C,  $L = 4$  mm,  $R = 1$  mm,  $\xi = -10^\circ$

In summary it can be concluded, that the probability of notch failure can be reduced by introducing a negative notch overlap angle  $\xi$  and/or by reducing the shear length  $L$ . A negative notch overlap reduces the triaxiality in the shear region with tendency to pressure loading in the beginning of the deformation process. A reduction of the shear length leads to increasing triaxiality in the shear zone, especially for larger strains. A practical solution to consider the sheet thickness dependent shear length is to use the above mentioned normalized thickness related shear length  $L/t$  at a constant level, preferably  $L/t = 2.7$  based on the results for  $t = 1.5$  mm.

#### 4 Experimental investigations

Test series were performed with different shear zone parameter combinations. For all materials and sheet thicknesses the specimen geometries with  $R = 1$  mm,  $L = 4$  mm and  $\xi = 0^\circ$  as well as  $\xi = -10^\circ$  were tested under quasi-static loading conditions. Dependent on the numerical results additional shear parameter combinations were investigated. For an assessment of the specimen geometry concerning the suitability for shear characterization the following goals are identified as most important:

1. The fracture surface of the tested specimens should show no ears (e.g. Figure 8 left and middle). The fracture surface in Figure 8 left shows failure in the center of the notch resulting in the formation of ears during rupturing. Considering the triaxiality field in Figure 3 right, failure with ears

- occurs under tension loading. The fracture surface in Figure 8 in the middle is a requirement but no guarantee for shear failure, because fracture initiation in the notch root still may have occurred.
- SEM images should show a shear fracture surface without any dimples (e.g. Figure 8 right).
  - The strain paths in the shear zone on the surface of the specimen evaluated by digital image correlation (DIC) should show shear dominated deformation (e.g. Figure 9 left).

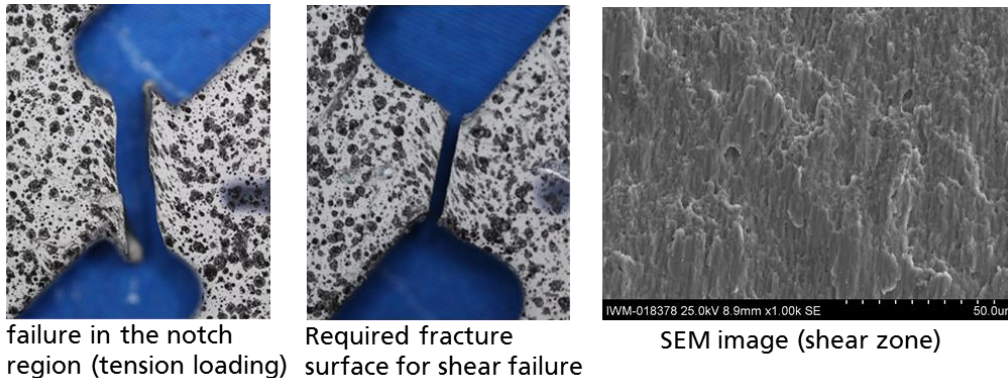


Fig.8: Quasi-static tested specimens of HCT980X+Z110MB (left:  $L = 3$  mm, middle:  $L = 4$  mm) and shear fracture area (near upper notch) (right)

Figure 9 shows strain paths in the center of the shear zone for different shear geometries tested on HCT780C with a sheet thickness of 1.5 mm. The equivalent v. Mises strain determined by DIC [15] is plotted against the parameter  $\alpha = \varphi_1/\varphi_2$  ( $\varphi_1 =$  major strain,  $\varphi_2 =$  minor strain). All investigated specimens show nearly a linear strain path at  $\alpha \sim -1$  (shear deformation). The specimen with  $L = 4$  mm and  $\xi = -9.48^\circ$  ( $e = -1$  mm) shows the largest equivalent strain up to failure. Judged by these experimental results this is a preferred specimen geometry for HCT780C ( $L/t = 2.7$ ). For analogous experiments leading to a fracture surface according to goal 1 (Figure 8 middle) strain paths in the center of the shear zone were determined by DIC. The preferred geometries and the results for the maximum strain before fracture are given in Figure 10 and in Table 2 in chapter 5. For strain rate dependent shear tests on HX340LAD strain paths are shown for the optimized geometry (coloured curves) and for the basic geometry (grey curve) in the right diagram in Figure 9. Even if under quasi-static loading failure initiation occurred in the upper notch, the optimized geometry (green curve) leads to larger strains before fracture initiation compared to the basic geometry.

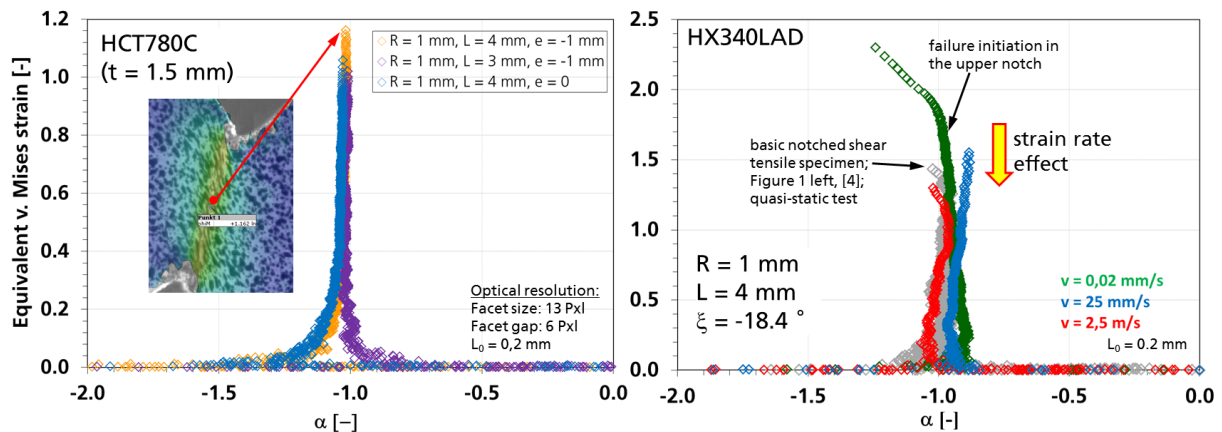


Fig.9: Strain paths in the shear zone evaluated by DIC [14], left for HCT780C ( $t = 1,5$  mm), right for HX340LAD at different strain rates

In Figure 10 left the results for the maximum equivalent strain in the shear zone immediately before fracture, obtained by DIC with optimized shear specimen geometries, are shown for the investigated AHSS with  $t = 1.5/1.4$  mm. The DIC strains are evaluated with  $L_0 = 0.2$  mm as medium values for 2-3 tests. For HCT980X+Z110MB and HX340LAD the maximum strain values obtained with the optimized geometries surpass the previous results obtained with the basic specimen geometry.

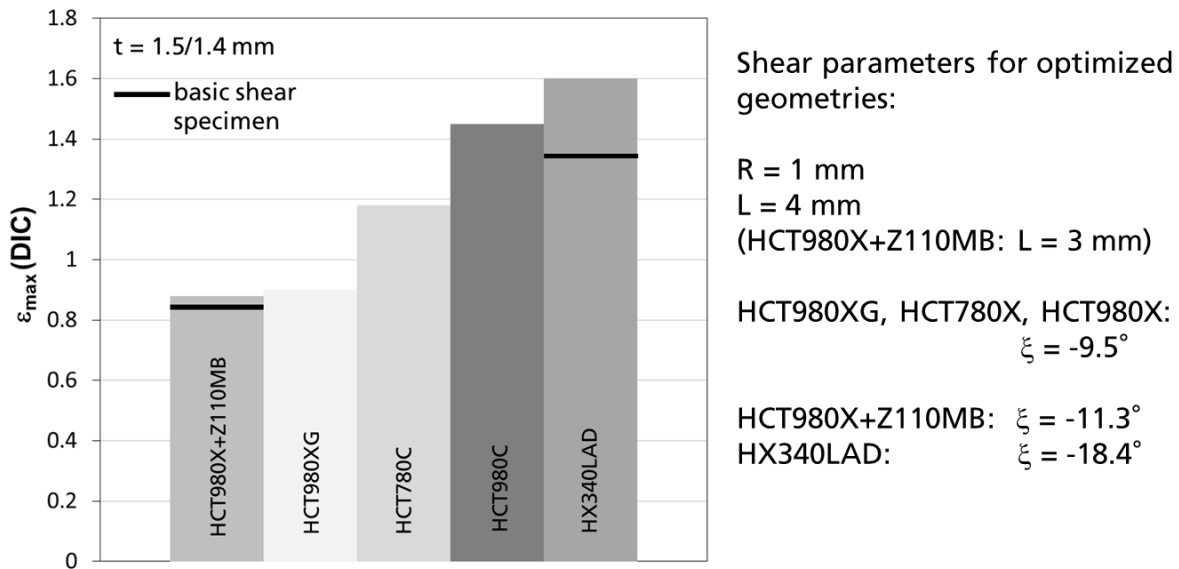


Fig.10: Maximum equivalent strain evaluated by DIC [14] reached by optimized and basic shear specimens for different AHSS with  $t = 1.5/1.4$  mm according to Table 1

An important impact on shear failure has the clamping configuration. To detect strain rate effects under shear loading, the same test setup is used for the quasi-static shear testing regime as it is used for high speed shear tension tests. Therefore the tests were performed with a high speed testing machine and with a rotatable clamping, which principally allows horizontal displacement of the specimen. To investigate effects of the specimen clamping on the shear deformation additional specimen geometries are tested with a fixed clamping without horizontal translationally degree of freedom. The fixed clamping leads for the optimized shear specimen geometries to the formation of ears, which indicates a possible tensile dominated initial fracturing in the notch region. Therefore, for a representative shear characterization with asymmetric notched shear tensile specimens a clamping with a horizontal translationally degree of freedom is necessary.

### 5 Material dependent design of notched shear tensile specimens

The numerical and experimental investigations with notched shear tensile specimens show the following results:

- Based on a numerical preliminary study a notch radius of  $R = 1$  mm is suitable.
- For a sheet thickness of  $t = 1.5$  mm the shear length  $L = 4$  mm is suggested. This was successful for all investigated materials except HCT980X+Z110MB, which shows a fracture surface with ears. In this case  $L = 3$  mm was successful and is proposed.
- The influence of the sheet thickness on the favorable shear zone parameters is taken into account by a thickness related shear length  $L/t = 2.7$ .
- The suitable negative notch overlap angle  $\xi$  shows a dependency on the mechanical values uniform strain  $A_g$  (before necking) and  $n$ -value  $n_{2-Ag}$  (hardening) according to Table 2. The materials are ordered by increasing  $A_g$  and increasing  $n_{2-Ag}$ .

Material	$R_{p0.2}$ [MPa]	$R_m$ [MPa]	$A_g$ [%]	$n_{2-Ag}$	$\xi_{exp}$ [°]	$\xi_{sim}$ [°]
HCT980C	890	1003	5.1	0.057	-9.5	-10
HCT980XG	759	1049	7.1	0.081	-9.5/-11.3	-10
HCT780C	689	878	8.4	0.094	-9.5	-10
HCT980X+Z110MB	683	1007	10.3	0.132	-11.3	-11.3
HX340LAD	390	461	17.4	0.149	-18.4	-18.4

Table 2: Mechanical values and suitable  $\xi$ -values for the investigated materials with sheet thickness 1.5/1.4 mm (perpendicular to rolling direction).

The suitable values for the  $\xi$ -angle obtained by the experimental and numerical investigations are also documented in Table 2. For a recommendation concerning suitable shear zone parameters based on material properties, only geometry independent technical values are reliable. Therefore values concerning the post-necking phase like the fracture strain  $A_{20mm}$ , are not listed in Table 2. With increasing  $A_g$  and increasing  $n_{2-Ag}$  a larger negative angle  $\xi$  is necessary, while the yield strength  $R_{p0.2}$  and the ultimate strength  $R_m$  don't correspond to  $\xi$ . In the following recommendation the  $\xi$ -angle is related to the strain hardening value  $n_{2-Ag}$  because of the detected batch and geometry independency of this material parameter [16,17]. An important goal in the shear characterization of different materials is to use less different shear specimen geometries as possible. Therefore the materials are clustered in three groups based on the n-values as it is described in the following recommendation.

For complex- and dual phase steel sheets as well as for microalloyed steel sheets with a sheet thickness  $t$  of  $1 \text{ mm} \leq t \leq 2 \text{ mm}$  the following recommendation for suitable shear parameters is given:

1.  $R = 1 \text{ mm}$
2.  $L = 2.7 t$
3.  $n_{2-Ag} < 0.1$ :  $\xi = -10^\circ$   
 $0.1 \leq n_{2-Ag} < 0.15$ :  $\xi = -15^\circ$   
 $n_{2-Ag} \geq 0.15$ :  $\xi = -20^\circ$

This recommendation is validated with two more steel sheets, a press hardened steel 22MnB5/AS and an additional microalloyed steel HC420LA, as well as alloys of copper CuDHP and aluminum Al1050. Therefore a wide range of strength and strain hardening is covered as Al1050 has nearly no strain hardening with n-values  $< 0.01$  and CuDHP has large strain hardening with n-values  $> 0.2$ . In the diagram in Figure 11 on the left side, the engineering stress strain curves are shown for the additional materials in relation to those explored for the geometry design recommendation (grey curves). The shear specimens are designed according to the recommendation above and examples of the tested specimens are shown in Figure 11 on the right. All specimens show a fracture surface without ears. Therefore the necessary requirement for shear failure is fulfilled. Especially the shear specimen of Al1050 with  $t = 2 \text{ mm}$  shows a large shear fracture angle of nearly  $90^\circ$ .

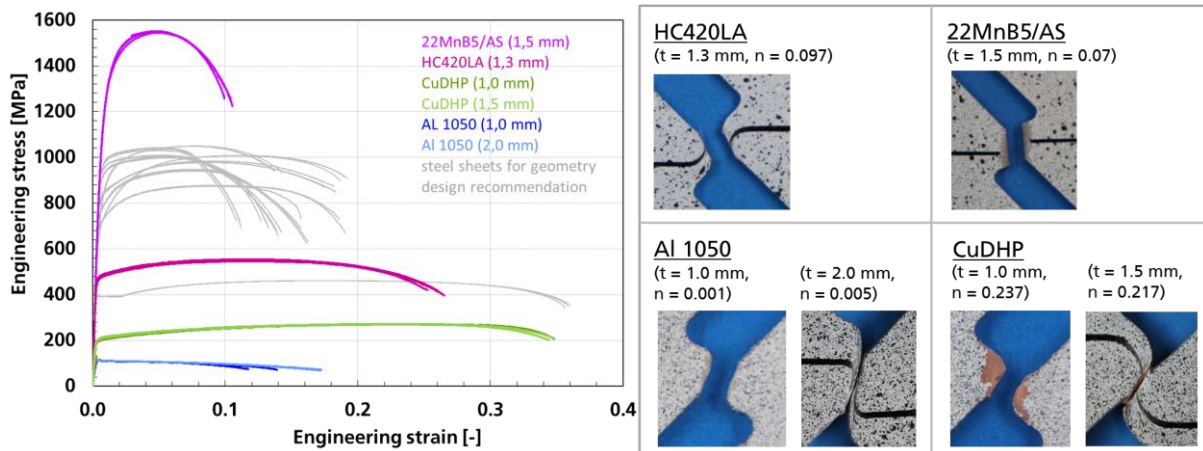


Fig.11: Engineering stress strain curves (left) and tested shear specimens (right) for validation

## 6 Strain rate dependent shear characterization

A strain rate dependent shear characterization is performed with the material dependent optimized asymmetric notched shear tensile specimen geometries with  $R = 1 \text{ mm}$  and  $L = 4 \text{ mm}$  (HX340LAD) and  $L = 3 \text{ mm}$  (HCT980X +Z110MB). The negative notch overlap angle  $\xi$  is chosen according to Table 2 ( $\xi_{exp}$ ). Figure 12 shows the normalized force displacement curves for three test speeds. For both materials the experimental results at 2.5 m/s show larger forces compared to the tests at smaller test speeds. With increasing test speed the displacement up to fracture decreases according to previous investigations with other shear specimen geometries [4]. The local fracture strain was determined by DIC using the equivalent strain for a facet in the shear zone at largest strain level immediately before fracture and with a nearly proportional strain path (e.g. Figure 9 right). A local gauge length of  $L_0 = 0.2 \text{ mm}$  was used.

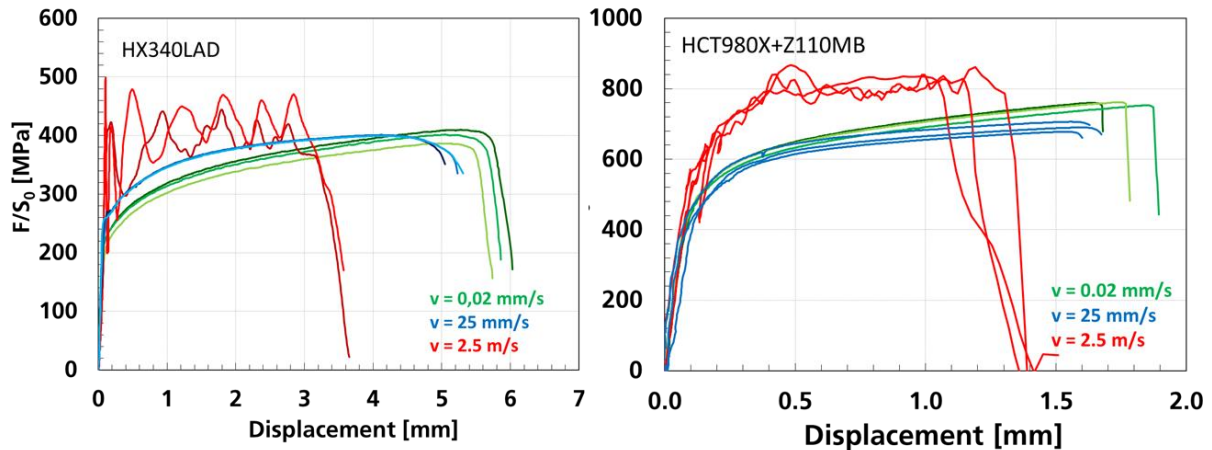


Fig.12: Influence of test speed on normalized force displacement curves, left HX340LAD, right HCT980X+Z110MB

In Figure 13 the failure curves for the two materials determined in previous investigations [4] are supplemented by the improved shear failure points. The failure strains in Figure 13 are determined by DIC and plotted against the average triaxiality determined by FE-simulation. For the previous investigations the results for triaxiality are taken from [18], for the supplemented shear failure points triaxiality is determined by FE-simulation described in chapter 3.

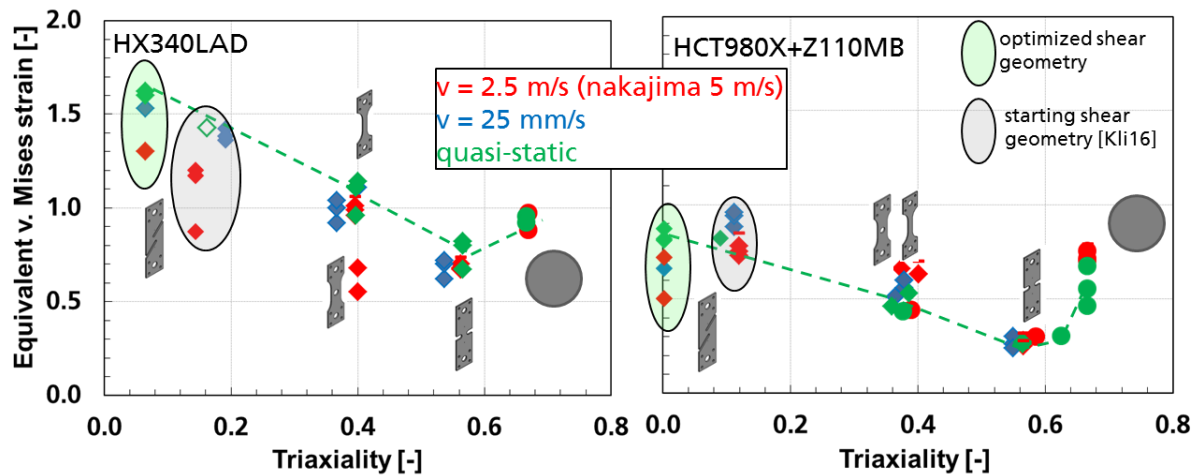


Fig.13: Influence of test speed on failure strain (DIC) against triaxiality (FE) including results of optimized shear geometries, left HX340LAD, right HCT980X+Z110MB.

The new shear specimens show the common known negative strain rate effect concerning the shear failure strains for both investigated materials. For HX340LAD the new shear specimen leads to shear failure points at larger strain values and at triaxialities closer to zero compared with the basic shear specimen geometry used in the past (Figure 1 left). This is a significant improvement in shear characterization. For HCT980X+Z110MB the new shear specimen doesn't show larger strains in comparison to previous results, but the triaxiality is shifted to smaller values closer to zero. So also for the dual phase steel this is an improvement in shear characterization.

## 7 Summary

For a strain rate dependent shear characterization of advanced high strength steels (AHSS) with notched shear tensile specimens the shear zone parameters notch radius, shear length and notch overlap angle are optimized with the goal to improve a shear dominated loading path and an initial shear dominated rupture. The optimized geometrical parameters of the specimens are dependent only on the sheet thickness and the strain hardening of the material. The whole design procedure for improved shear specimen geometries are based on numerical simulations and extensive experimental investigations. The optimized specimen geometries with a constant notch radius of  $R = 1$  mm and a

sheet thickness dependent shear length  $L = 2.7 t$  are clustered in three categories with different negative notch overlap angles  $\xi$ . The optimized specimen geometries lead to larger shear strains immediately before failure and smaller stress triaxialities close to zero. They reduce the probability of notch failure compared to previous investigations under the requirement of a clamping which allows horizontal translational displacement. The strain rate dependent shear characterization of HCT980X+Z110MB and HX340LAD lead to a negative strain rate effect concerning to local and global failure strain.

## 8 Acknowledgements

The AiF project No. 18943 N/1 "Strain rate dependent deformation- and failure behavior of thin steel sheets under shear loading" is accompanied and funded by the Research Associations for Automotive Engineering (FAT), Steel Application (FOSTA) and the German Federation of Industrial Research Associations e.V. (AiF) with budget funds of the "Federal Ministry for Economic Affairs and Energy" (BMWi). We gratefully acknowledge all Research Associations as well as all industrial partners for funding and supporting this project.

## 9 Literature

- [1] El-Magd, E., Gese, H., Tham, R., Hooputra, H., Werner, H.: Fracture Criteria for Automobile Crashworthiness Simulation of Wrought Aluminium Alloy Components; Mat-wiss. u. Werkstofftech. 32, 2001, pp. 712-724
- [2] Peirs, J., Verleysen, P., Degrieck, J.: Novel technique for static and dynamic shear testing of Ti6Al4V sheet, Experimental Me-chanics., Vol. 52, Iss. 7, 2012, pp. 729-741
- [3] Roth, C-C, Mohr, D, Experimental investigation on shear fracture at high strain rates, 11th Conf. on Mech. And Phys. Behavior of Materials under Dynamic Loads (DYMAT), Lugano, 2015
- [4] Klitschke, S, Böhme, W, Deformation and damage behavior of lightweight steels at highrate multiaxial loading, Mat. Test. 58 3: 2016, pp. 173-181, doi: 10.3139/ 120.110836
- [5] Behrens, B.-A., Bouguecha, A., Vucetic, M., Peshekhodov, I.: An experimental-numerical method to characterise formability of sheet metals in a wide range of stress states with the help of a tensile-shear test on new butterfly specimens, Int. Scientific and Tech. Conf. on Adv. Metal. Materials and Techn. 2013
- [6] Authenrieth, H., Schulze. V., Herzig, N., Meyer, L.W., Ductile failure model for the description of AISI 1045 behavior under different loading conditions, Mech. Time-Depend. Mater. Vol. 13, 2009, pp. 215-231.
- [7] Yin, Q., Verfestigungs- und Schädigungsverhalten von Blechwerkstoffen im ebenen Torsionsversuch, Dissertation, Technische Universität Dortmund, 2014
- [8] Sun, D.-Z., Feucht, M., Klamser, H.: Versagensverhalten von verschiedenen Werkstoffen unter mehrachsiger Belastung; 6. Freiburg Workshop crashMAT, Freiburg, 2012
- [9] Miyauchi, K., A proposal for a planar simple shear test in sheet metals, Sci. Papers RIKEN 81, 1984, pp. 27-42
- [10] Merklein, M., Biasutti, M., A contribution to the optimisation of a simple shear test, Key Engineering Materials, 2009, pp. 410-411
- [11] Riemensperger, D., Ekic, D., Lauterbach, B.: Optimierte Zugproben zur Schädigungsmodellierung mit Schalenelementen, VDI-Bericht 2224, 2014, pp. 237-249
- [12] Böhme, W., Reith, T., Hohe, J: New notched shear tensile specimen with negative notch overlap, unpublished results of IWM, 2011
- [13] Böhme, W.: FAT-Richtlinie »Dynamische Werkstoffkennwerte für die Crashesimulation«, Zeitschrift Materialprüfung, Materials Testing, Carl Hanser Verlag, München, Vol.50 (4), 2008, pp. 199 - 205
- [14] LS-DYNA, User Manual / Theory Manual R10.0 (October 2017), Livermore Software Technology Cooperation, <http://www.lstc.com/download/manuals>
- [15] <http://www.gom.com/de/messsysteme/aramis.html>
- [16] Heibel, S., Dettinger, T., Nester, W., Clausmeyer, T., Tekkaya, A.E., Damage Mechanisms and Mechanical Properties of High-Strength Multiphase Steels, Materials, 2018, 11, 761; doi:10.3390/ ma11050761
- [17] Richter, H., Test report of flow curve testing (private information), Thyssenkrupp AG, 2018
- [18] Trondl, A., et al. 2015. Verformungs- und Versagensverhalten von Stählen für den Automobilbau unter crashartiger mehrachsiger Belastung, A 278/P979, Stiftungs-Nr. S24/10195/12, Schlussbericht 1235/2015, 2015